

## High-pressure ultrasonic investigation of order-disorder phenomena in $\text{NH}_4\text{Br}$

C. W. Garland, R. C. Leung, and F. P. Missell\*

Department of Chemistry and Center for Materials Science and Engineering, Massachusetts Institute of Technology, Cambridge, Massachusetts 02139

(Received 25 May 1978)

The adiabatic elastic constants  $C_{11}$ ,  $C_{44}$ ,  $C' \equiv (C_{11} - C_{12})/2$ , and the [100] longitudinal attenuation have been measured in single-crystal  $\text{NH}_4\text{Br}$ . The  $C_{44}$  data establish that there is a multicritical point along the cubic order-disorder transition line at 3.2 kbar and 215.8 K. The  $C_{11}$  and  $C'$  data indicate a close analogy between the behavior of  $\text{NH}_4\text{Cl}$  at 1 atm and the behavior of  $\text{NH}_4\text{Br}$  near its disorder-cubic-order-tetragonal-order triple point. The attenuation data strengthen this analogy and show a strong pressure dependence as  $p$  varies from 1 atm (tetragonal ordering) to the triplet-point pressure to 3.25 kbar (cubic ordering).

### I. INTRODUCTION

Both  $\text{NH}_4\text{Cl}$  and  $\text{NH}_4\text{Br}$  crystals undergo  $\lambda$ -type order-disorder transitions involving the relative orientations of the tetrahedral  $\text{NH}_4^+$  ions. In the case of  $\text{NH}_4\text{Cl}$ , there is a single transition line  $T_c(p)$  between the disordered phase and a "ferro-ordered" phase, both of which have a CsCl-type cubic structure.<sup>1</sup> The phase diagram of  $\text{NH}_4\text{Br}$ , as shown in Fig. 1, is more complicated. An "antiferro-ordered" phase occurs at low pressures, and this new phase involves a small tetragonal distortion with oppositely oriented chains of  $\text{NH}_4^+$  lying along the tetragonal axis.<sup>2</sup> At one time it was thought that two different cubic-ordered phases existed for  $\text{NH}_4\text{Br}$ ,<sup>3,4</sup> but recent high-pressure neutron,<sup>5</sup> Raman,<sup>6</sup> and NMR<sup>7</sup> studies have established that there is only one. A rationalization of this  $\text{NH}_4\text{Br}$  phase diagram is provided by theoretical models<sup>8</sup> in which there are two competing interactions between the  $\text{NH}_4^+$  ions—a direct octopole-octopole interaction (which favors ferro-ordering) and an indirect interaction involving the polarizable halide ion (which favors antiferro-ordering).

The point at  $\sim 1.7$  kbar and  $\sim 201$  K where the two order-disorder lines D-O(T) and D-O(C) meet with the first-order O(C)-O(T) phase line (see Fig. 1) is closely analogous to the tetracritical and bicritical points which can occur in antiferromagnetic systems.<sup>9</sup> Since there are small first-order instabilities along both D-O lines near this point, we shall refer to this point as a triple point rather than designating it as a special sort of multicritical point.

The order-disorder transition in  $\text{NH}_4\text{Cl}$  exhibits a small first-order instability at low pressures, but the transition becomes continuous above 1.5 kbar.<sup>1,10</sup> Thus there is a high-pressure "multicritical" point in  $\text{NH}_4\text{Cl}$ . One objective of the present work is to establish the location of

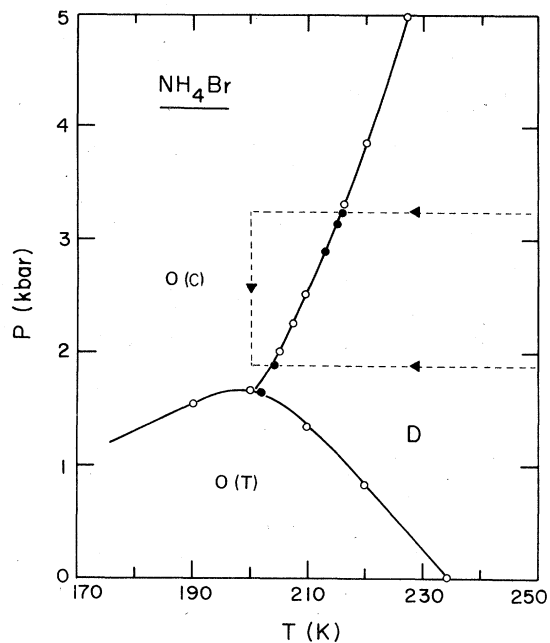


FIG. 1. Phase diagram for  $\text{NH}_4\text{Br}$ . Solid circles indicate transition points determined in this work; open circles represent data taken from Ref. 3. Phases D and O(C) are disordered and ordered cubic phases with the CsCl structure; O(T) is an ordered tetragonal phase. The dashed lines indicate the paths along which  $C_{11}$  measurements have been made.

the corresponding multicritical point along the D-O(C) transition line in  $\text{NH}_4\text{Br}$ , using the shear elastic constant  $C_{44}$  as a probe. A second objective is to measure the longitudinal elastic constant  $C_{11}$  as a function of  $T - T_c(p)$  along isobars at the multicritical pressure and at a pressure close to the triple-point pressure. This will augment previous ultrasonic velocity measurements in  $\text{NH}_4\text{Br}$ ,<sup>3,11</sup> and will permit direct comparison with analogous  $C_{11}$  data in  $\text{NH}_4\text{Cl}$ .<sup>12</sup> Additional comparisons will also be made for the

behavior of the shear constant  $C'$ . The third objective of this work is to determine the longitudinal attenuation at high pressures. This will allow a characterization of the changes in dynamical behavior on going from a region where indirect interactions are dominant (1 atm) to a region where direct and indirect interactions are equally important (triple-point pressure) to a region where direct octopole-octopole interactions dominate.<sup>8</sup>

## II. EXPERIMENTAL RESULTS

The ultrasonic techniques used in this investigation were essentially the same as those used previously in Refs. 3 and 11, except that two transducers were used. Velocity measurements were made at 10 MHz with the pulse-superposition method. For longitudinal waves at  $\Delta T = |T - T_c| < 2.5$  K, the attenuation was too high for this method and changes in velocity were followed by measuring the change in delay time for a given rf peak in the directly transmitted signal. Attenuation measurements were made with Matec pulse-comparison equipment. Corrections have been made for the pressure and temperature dependence of the density and acoustical path length,<sup>3</sup> but such corrections have a very small effect on the elastic constants ( $\approx 1\%$ ).

Hydrostatic pressures, obtained using nitrogen gas, were measured with a calibrated manganin gauge. Along an isobar the pressure was held constant to within  $\pm 5$  bar and the absolute values are accurate to within  $\pm 10$  bar. Temperatures, as measured with a platinum resistance thermometer mounted on the exterior of the beryllium-copper pressure cell, were held constant to within  $\pm 50$  mK prior to making a measurement. Thermodynamic equilibrium was usually achieved within a period of  $\sim 30$  min, but very close to  $T_c$  (say  $|\Delta T| < 1$  K) it was necessary to wait for at least 60 min.

The  $\text{NH}_4\text{Br}$  single crystals used in this work were the same as those investigated in Ref. 11 (denoted there as Ib and II). After repolishing, the path lengths between a pair of parallel (100) faces on crystal Ib and (110) faces on crystal II were 0.8141 and 0.6077 cm at 20 °C. Transverse and longitudinal acoustical velocities  $u$  in the [100] direction are simply related to the elastic stiffness constants by  $C_{44} = \rho u_T^2$  and  $C_{11} = \rho u_L^2$ , where  $\rho$  is the mass density. For the [110] transverse wave with a [110] polarization,  $C' = \frac{1}{2}(C_{11} - C_{12}) = \rho u_T'^2$ .

*Transverse velocities.* The shear constant  $C_{44}$ , which follows the variation in the configurational energy and the volume,<sup>13,14</sup> is a good high-pres-

sure probe of the behavior in the immediate vicinity of the transition. It has been established by earlier work that the D-O (C) transition exhibits a small first-order discontinuity between the triple-point pressure and  $\sim 2.5$  kbar but the transition is continuous above 3.65 kbar.<sup>3,5</sup> Our  $C_{44}$  results shown in Fig. 2, indicate that the multicritical pressure lies slightly above 3 kbar. The  $C_{44}$  variations at 3.14 and 3.25 kbar are essentially identical, and neither indicate hysteresis or direct evidence of an isothermal discontinuity. In the case of data taken at 2.91 kbar, a very small discontinuous change was observed at 213.65 K on warming and at 213.5 K on cooling. On the basis of these results the multicritical point for this sample is taken to be 3.2 kbar and 215.8 K.

The shear constant  $C'$  has been studied at a single pressure (1.66 kbar) just below the triple-point pressure, and the results are shown in Fig. 3. This pressure region is of special interest because the  $C'$  wave shows an anomalous temperature variation and associated attenuation in the disordered phase at 1 atm but does not show these features at high pressures where only cubic ordering occurs.

*Longitudinal velocity.* The variation of the elastic constant  $C_{11}$  along three isobars is shown in Fig. 4. Note that the behavior of  $C_{11}$  on entering the tetragonal antiferro-ordered phase (isobar at  $p_1 = 1$  atm) is quite different from that on enter-

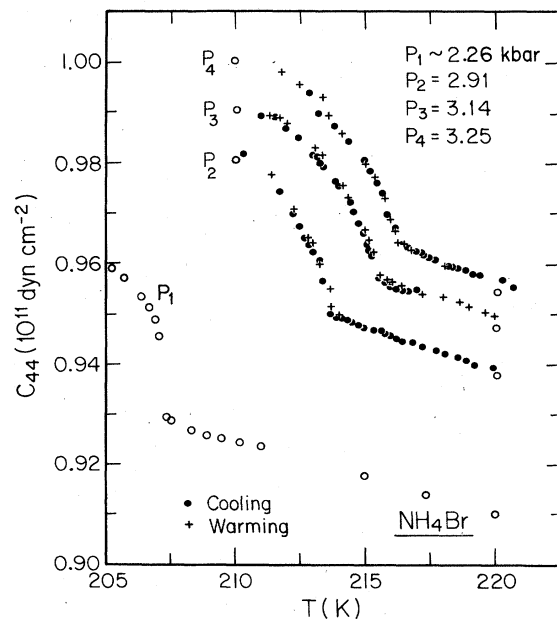


FIG. 2. Variation of  $C_{44}$  with temperature along several isobars. The open circles represent data taken from Ref. 3.

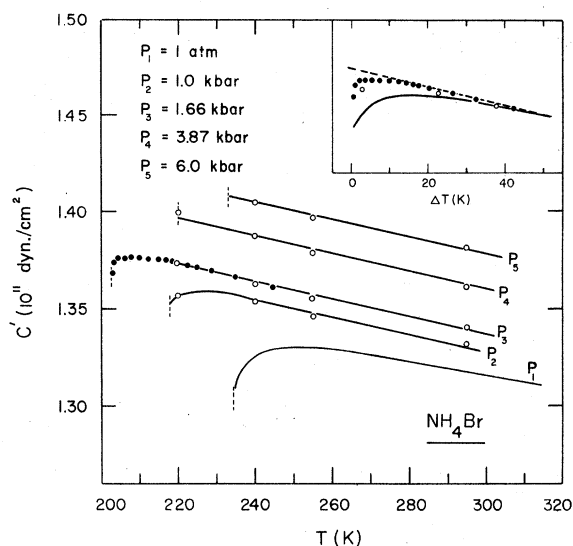


FIG. 3. Temperature variation of  $C'$  in the disordered phase along several isobars. The present measurements at 1.66 kbar are represented by the solid points. The open circles represent the available high-pressure data from Refs. 2 and 3. The line at 1 atm is the smooth-curve variation based on extensive data in Ref. 2; the other lines are merely guides for the eye. The transition temperature at each pressure is indicated by the vertical dashed line. The inset compares the shape of the  $C'$  variation as a function of  $\Delta T = T - T_c$  at 1 atm (solid line), 1 kbar (open circles), 1.66 kbar (filled circles), and both 3.87 and 6 kbar (dashed line).

ing the cubic ferro-ordered phase (isobar at  $p_3 = 3.25$  kbar). The new high-pressure results are in very good agreement with previous measurements<sup>2,3</sup> along widely spaced isotherms in the disordered phase. Values of  $C_{11}$  reported in Ref. 3 for the cubic-ordered phase must, however, be systematically reduced by  $\sim 4\%$ , corresponding to a change of 2 in the choice of  $n$  used in the pulse-superposition method.<sup>15</sup> Smooth-curve values of  $C_{11}$  and  $C_{44}$  are given in Table I.

It should be noted that the  $C_{11}$  values observed on cooling below the transition temperature at 1.88 kbar do not conform with the behavior expected for the ferro-ordered phase. Two independent runs, which were in excellent agreement above  $T_c$ , gave similar but not quite identical results just below  $T_c$ . In order to clarify the equilibrium value of  $C_{11}$  in the ordered phase at 1.88 kbar, measurements were made as a function of pressure at 200 K. This run was made by first cooling the crystal at 3.25 kbar and then decreasing the pressure (see Fig. 1). The  $C_{11}$  value obtained in this way at 1.88 kbar and 200 K is shown by the "+" symbol in Fig. 4 and Table I. On the basis of the observed  $C_{11}$  behavior in  $\text{NH}_4\text{Cl}$ ,<sup>12</sup> one would expect the equilibrium  $C_{11}$  values in the cubic-or-

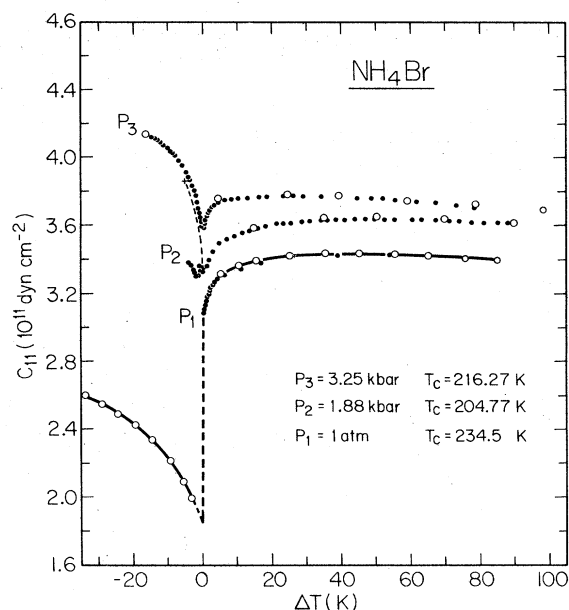


FIG. 4. Variation of  $C_{11}$  as a function of  $\Delta T = T - T_c$  along three isobars. The open circles represent data taken from Refs. 2, 3, and 10; the solid circles and the plus symbol represent data obtained in the present investigation.  $\text{NH}_4\text{Br}$  becomes antiferro-ordered at  $p_1$  and ferro-ordered at  $p_3$ ; see text for a discussion of the behavior at  $p_2$ .

dered phase at 1.88 kbar to follow the dashed curve in Fig. 4. We suggest that a metastable mixed phase containing both ferro- and antiferro-ordered domains was obtained on cooling at 1.88 kbar, and the observed  $C_{11}$  values shown in parentheses in Table I represent some sort of average of the values for the two ordered phases.

**Longitudinal attenuation.** The absorption coefficient  $\alpha$  of [100] longitudinal waves has been measured as a function of frequency, temperature, and pressure. Data were obtained at 10, 30, and 50 MHz for temperatures in the range  $20 \leq \Delta T \leq 100$  K and also at 70 MHz for  $\Delta T > 40$  K. Plots of  $\alpha$  vs  $f^2$  gave a family of straight lines with a common intercept  $\alpha_0 = 1.2$  dB cm<sup>-1</sup> at 1 atm, 2.5 dB cm<sup>-1</sup> at 1.88 kbar, and 3.4 dB cm<sup>-1</sup> at 3.25 kbar. Thus the attenuation consists of a relaxation contribution and a small background contribution  $\alpha_0$  which is independent of temperature and roughly linear in pressure.

The behavior of  $(\alpha - \alpha_0)/\omega^2$  in the disordered phase is shown in Fig. 5. For values of  $\Delta T$  less than  $\sim 20$  K, measurements could be made only at 10 and 30 MHz and  $(\alpha - \alpha_0)/\omega^2$  values are shown at both these frequencies. Near the transition temperature there are systematic differences between these two sets of values that can be explained in terms of a critical relaxation time  $\tau$  that grows

TABLE I. Smooth-curve values of  $C_{11}$  and  $C_{44}$  in units of  $10^{11}$  dyn  $\text{cm}^{-2}$ .

$p = 3.25$ kbar ( $T_c = 216.3$ K)					
$T$ (K)	$C_{11}$	$C_{44}$	$T$ (K)	$C_{11}$	
200	4.131	1.032	220	3.733	
205	4.065	1.020	230	3.764	
210	3.946	1.003	240	3.765	
212	3.865	0.997	250	3.757	
214	3.728	0.986	260	3.749	
216	3.580	0.969	270	3.739	
217	3.660	0.962	280	3.724	
218	3.704	0.960	290	3.708	
219	3.718	0.958	300	3.704	

$p = 1.88$ kbar ( $T_c = 204.8$ K)					
$T$ (K)	$C_{11}$	$T$ (K)	$C_{11}$	$T$ (K)	$C_{11}$
200	3.859 +	206	3.347	240	3.623
201	(3.365)	207	3.426	250	3.625
202	(3.326)	208	3.448	260	3.625
203	(3.304)	210	3.485	270	3.622
204	(3.355)	220	3.580	280	3.615
205	3.278	230	3.615	290	3.601

$T = 200$ K			
$p$ (kbar)	$C_{11}$	$p$ (kbar)	$C_{11}$
1.9	3.859	3.5	4.201
2.0	3.907	4.0	4.265
2.5	4.035	4.5	4.325
3.0	4.111	5.0	4.365

rapidly on approaching  $T_c$ . The variation of  $(\alpha - \alpha_0)/\omega^2$  in the cubic-ordered phase at 3.25 kbar is shown in Fig. 6. The value used for  $\alpha_0$  is the same as that in the disordered phase.

**Transverse attenuation.** There is no critical attenuation associated with  $C_{44}$ , but the [110] transverse wave with [110] polarization ( $C'$  wave) does show critical attenuation in  $\text{NH}_4\text{Br}$  at 1 atm.<sup>11</sup> Since this is in contrast with the absence of  $C'$  attenuation in  $\text{NH}_4\text{Cl}$ , it was of the interest to look at the  $C'$  attenuation in  $\text{NH}_4\text{Br}$  near the triple-point pressure. The  $C'$  attenuation at 1.88 kbar was small and showed absolutely no variation with temperature over the range  $1 \text{ K} < \Delta T < 80 \text{ K}$ , thus ruling out critical shear attenuation at this pressure. At 1.66 kbar the  $C'$  attenuation is larger: the value  $(\alpha - \alpha_0)/\omega^2 = 2.1 \times 10^{-17} \text{ sec}^2 \text{ cm}^{-1}$  obtained at  $\Delta T = 2.2 \text{ K}$  is about two-thirds of the 1-atm value at this  $\Delta T$ . However, the temperature variation close to  $T_c$  is rather mild [doubling  $\Delta T$  to 4.4 K decreases  $(\alpha - \alpha_0)/\omega^2$  to  $1.65 \times 10^{-17} \text{ sec}^2 \text{ cm}^{-1}$ ].

### III. DISCUSSION

**Static aspects.** It has been proposed<sup>5</sup> that the order-disorder phase transitions in  $\text{NH}_4\text{Cl}$ ,  $\text{ND}_4\text{Cl}$ ,  $\text{NH}_4\text{Br}$ , and  $\text{ND}_4\text{Br}$  can all be understood in terms of a common phase diagram involving a triple point and a multicritical point along the D-O (C) line. Now that the location of this multicritical point has been established for  $\text{NH}_4\text{Br}$ , it is possible to carry out a quantitative test of this suggestion. Figure 7 shows the master phase diagram obtained by plotting  $p - p^*$  vs  $T - T^*$ , where  $p^*$  and  $T^*$  denote the pressure and temperature of the D-O (C) multicritical point. The  $p^*$ ,  $T^*$  values listed in Fig. 7 were taken from Ref. 1 for  $\text{NH}_4\text{Cl}$  and Ref. 16 for  $\text{ND}_4\text{Cl}$ . In the case of  $\text{ND}_4\text{Br}$ , we have chosen  $p^* = 2.2$  kbar in order to secure the best fit to the master diagram. This choice is consistent with neutron diffraction results<sup>5</sup> which indicate that the transition is discontinuous at 2 kbar but continuous above 3 kbar.

Figure 7 clearly indicates that these four salts can be well represented by a single phase diagram. As a result, one would expect the behavior of  $\text{NH}_4\text{Cl}$  at 1 atm to be very similar to that of  $\text{NH}_4\text{Br}$  slightly above the triple-point pressure, where the influence of indirect interactions is still strong (see also Ref. 17). The  $C_{11}$  data provide a strong confirmation of this correspondence between  $\text{NH}_4\text{Cl}$  and  $\text{NH}_4\text{Br}$ , as shown in Fig. 8. However, the comparison at the multicritical pressures does not show as good a quantitative correspondence. The character of the change in  $\Delta C_{11}$  on increasing  $p$  to the multicritical pressure is very similar (see also Ref. 18), but the  $\text{NH}_4\text{Br}$  and  $\text{NH}_4\text{Cl}$  curves do not have exactly the same shape.

**Dynamical aspects.** It can be seen from Fig. 5 that there is a noncritical attenuation that is dominant at very large values of  $\Delta T$ . This contribution is quadratic in frequency over the investigated 10–70 MHz range, independent of temperature over the range  $50 < \Delta T < 100$ , and independent of pressure. We shall assume that the total attenuation is given over the entire range of  $\Delta T$  by

$$\alpha = \alpha_0(p) + \alpha_1(\omega) + \alpha_c(\omega, p, \Delta T), \quad (1)$$

where  $\alpha_0$  is the frequency-independent background attenuation described previously,  $\alpha_1$  is a noncritical attenuation independent of  $p$  and  $T$  ( $\alpha_1/\omega^2 = 0.2 \times 10^{-17} \text{ cm}^{-1} \text{ sec}^2$ ), and  $\alpha_c$  is the critical attenuation. Fortunately, the noncritical attenuation is quite small and the correction for this contribution has a significant effect only at 3.25 kbar. The magnitude of the noncritical contribu-

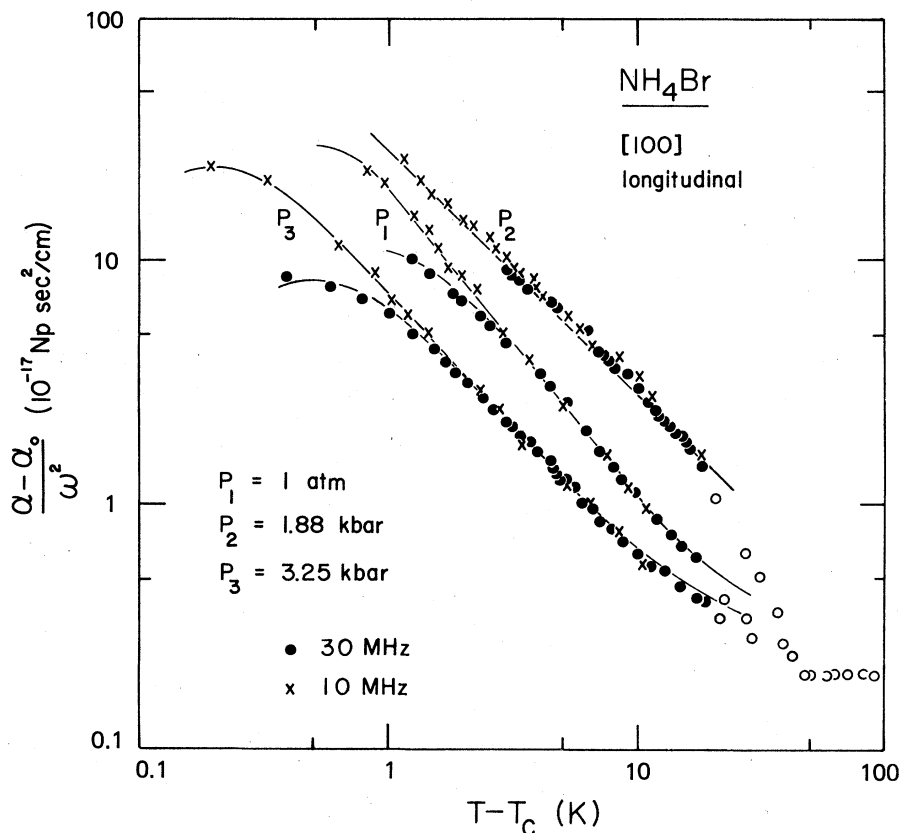


FIG. 5. Log-log plots of  $(\alpha - \alpha_0)/\omega^2$  vs  $\Delta T$  for the longitudinal attenuation in the disordered phase along several isobars. The open circles represent values obtained from the slopes of  $\alpha$  vs  $f^2$  plots. The lines represent fits with Eq. (2) using critical relaxation times  $\tau$  that diverge like  $t^{-\theta}$ .

tion  $\alpha_1$  is not known in the ordered phase since data are not available far below  $T_c$ . In evaluating the variation of  $\alpha_c$  in the ordered phase, it will be assumed that  $\alpha_1$  has the same value as above  $T_c$ , but this assumption has very little effect on the result.

The attenuation observed at 1 atm is in excellent agreement with previous values: both the magnitude and the temperature dependence are essentially identical with those reported in Ref. 11. The new data extend to larger  $\Delta T$ , revealing the "plateau" associated with the noncritical  $\alpha_1$  contribution; and they also show the systematic deviations from a quadratic frequency dependence close to  $T_c$ .

A review of all the available dynamical information<sup>19</sup> on  $\text{NH}_4\text{Cl}$ ,  $\text{ND}_4\text{Cl}$ , and  $\text{NH}_4\text{Br}$  shows that the critical longitudinal attenuation  $\alpha_c$  can be well represented up to  $\omega\tau \approx 1$  by a single relaxation formula with a constant relaxation strength. Thus we have for  $(\alpha - \alpha_0)/\omega^2$ , in units of  $\text{Np cm}^{-1} \text{sec}^2$ ,

$$\frac{\alpha - \alpha_0}{\omega^2} = \frac{\alpha_1}{\omega^2} + \frac{\alpha_c}{\omega^2} = 0.2 \times 10^{-17} + \frac{C\tau}{1 + \omega^2\tau^2}, \quad (2)$$

where  $\tau$  is the critical relaxation time. In the region close to the transition, the acoustical re-

laxation rate  $1/\tau$  can be correlated to the critical rate of order-parameter relaxation  $\omega_p \sim \xi^{-z} \sim t^{-\nu}$ , where  $\xi$  is the correlation length,  $t$  is the reduced temperature  $\Delta T/T_c$ ,  $\nu$  is a static critical exponent, and  $z$  is the dynamical critical exponent.<sup>20,21</sup> Therefore, we wish to test the possibility of fitting our attenuation data with Eq. (2) using a simple power law of the form  $\tau = at^{-\theta}$ .

As shown in Figs. 5 and 6, the observed  $(\alpha - \alpha_0)/\omega^2$  values can be well represented by Eq. (2). For the disordered phase at 1 atm and 3.25 kbar, we have used  $C(1 \text{ atm}) = 3.75 \times 10^{-8} \text{ sec cm}^{-1}$  and  $\tau(1 \text{ atm}) = 3.22 \times 10^{-12} t^{-1.38} \text{ sec}$ ,  $C(3.25 \text{ kbar}) = 2.95 \times 10^{-8} \text{ sec cm}^{-1}$ , and  $\tau(3.25 \text{ kbar}) = 4.14 \times 10^{-12} t^{-1.20} \text{ sec}$ . In the case of the disordered phase at 1.88 kbar and the ordered phase at 3.25 kbar, all our data lie in the range for which  $\omega^2\tau^2 \ll 1$  and we can only specify the  $C\tau$  product:  $C\tau(1.88 \text{ kbar}) = 13.6 \times 10^{-19} t^{-1.00} \text{ sec}^2 \text{ cm}^{-1}$  and  $C\tau(3.25 \text{ kbar, ordered phase}) = 2.88 \times 10^{-19} t^{-1.30} \text{ sec}^2 \text{ cm}^{-1}$ .<sup>22</sup> The slight deviations between observed  $(\alpha - \alpha_0)/\omega^2$  values and the calculated curves for  $\Delta T > 20 \text{ K}$  indicate a breakdown in the power-law behavior for  $\tau$  at large  $\Delta T$  values,<sup>19</sup> but we are interested here in the asymptotic behavior close to  $T_c$ .

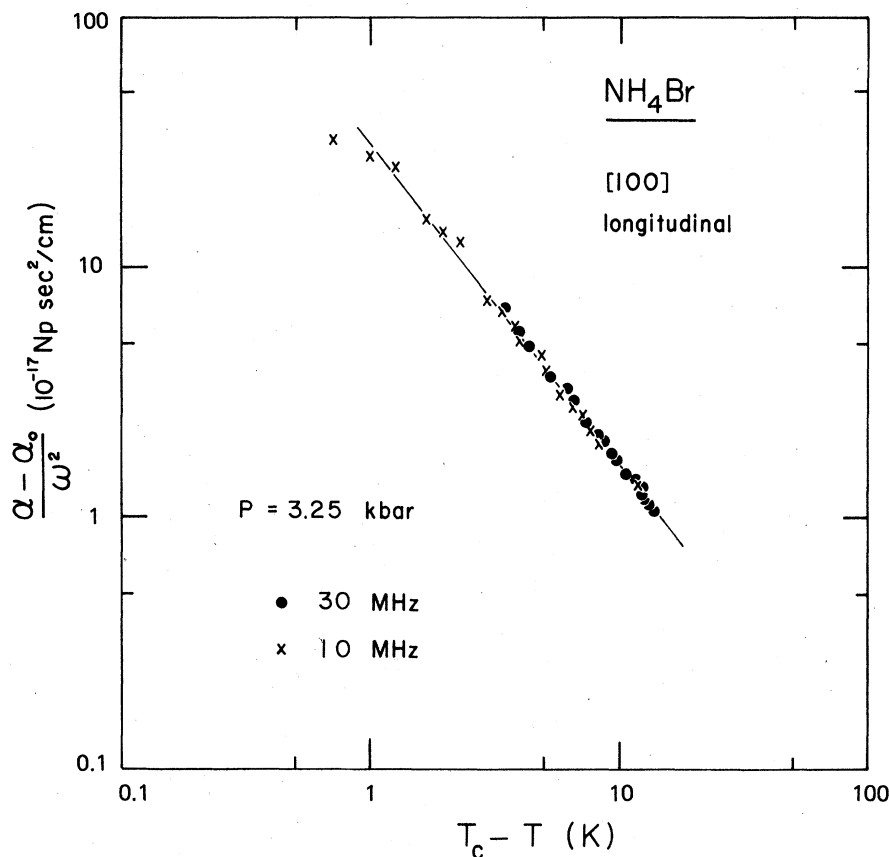


FIG. 6. Log-log plot of  $(\alpha - \alpha_0)/\omega^2$  vs  $\Delta T$  in the cubic-ordered phase at  $p_3 = 3.25$  kbar. The line represents a fit with Eq. (2) when  $\omega^2\tau^2 \ll 1$  and  $C\tau \sim t^{-1.3}$ .

Any comparison between the experimental critical exponents  $\theta$  and theoretical values for  $z\nu$  requires a specification of the dynamical model. Although the complete Hamiltonian and the equations of motion are not established for  $\text{NH}_4\text{Br}$ , the general character of this system suggests comparison with Hohenberg and Halperin's model A.<sup>21</sup> This purely relaxational model for an  $n$ -component order parameter is based on dissipative equations of motion with no conserved quantities. The resulting dynamical exponent is  $z \approx 2.05$  for a second-order critical point and  $z = 2$  for a tricritical or higher-order critical point.<sup>21,23</sup>

The isobar at 1 atm corresponds to a region of the  $\text{NH}_4\text{Br}$  phase diagram where fluctuations in the three-component antiferro-order parameter should be dominant. Thus we shall compare  $\theta(1 \text{ atm}) = 1.38 \pm 0.03$  with theoretical  $z\nu$  values at an  $n=3$  fixed point in  $d=3$  dimensions. For model A,  $z\nu = 1.43$  for an isotropic  $n=3$  Heisenberg fixed point and  $z\nu \approx 1.37$  for an  $n=3$  cubic fixed point,<sup>20</sup> both of which are in fair agreement with  $\theta(1 \text{ atm})$ .

The attenuation observed at 1.88 kbar shows a different temperature dependence,  $\theta(1.88 \text{ kbar})$

$= 1.00 \pm 0.03$ , which agrees with the behavior in  $\text{NH}_4\text{Cl}$  at 1 atm.<sup>12,19</sup> This correspondence in the dynamical behavior strengthens the analogy between  $\text{NH}_4\text{Cl}$  at 1 atm and  $\text{NH}_4\text{Br}$  near its triple-point pressure, discussed above in terms of the static behavior. The  $\theta(1.88 \text{ kbar})$  value does not correspond to any theoretical  $z\nu$  values for  $n$ -component spin models near a second-order transition,<sup>21</sup> but it does agree with the critical slowing down predicted by conventional theory (for which  $z = 2$  and  $\nu = \frac{1}{2}$ ). Since conventional theory should be appropriate for kinetic model A near higher-order critical points (where the marginal dimensionality  $d^* \leq 3$ ),<sup>23</sup> our results are consistent with the idea that the triple point is a special type of multicritical point.

Finally, the attenuation observed in the disordered phase at 3.25 kbar can be compared with that reported in  $\text{NH}_4\text{Cl}$  near its multicritical pressure of 1.5 kbar.<sup>12</sup> The latter data are reported to yield an exponent  $\theta = 1.1 \pm 0.1$ , in contrast to our  $\theta(3.25 \text{ kbar}) = 1.20 \pm 0.05$ . However, the high-pressure  $\text{NH}_4\text{Cl}$  data were obtained only at 15 MHz and showed a moderate amount of scatter, while our  $\theta(3.25 \text{ kbar})$  value is the one  $\text{NH}_4\text{Br}$  exponent that is sensitive to the choice of

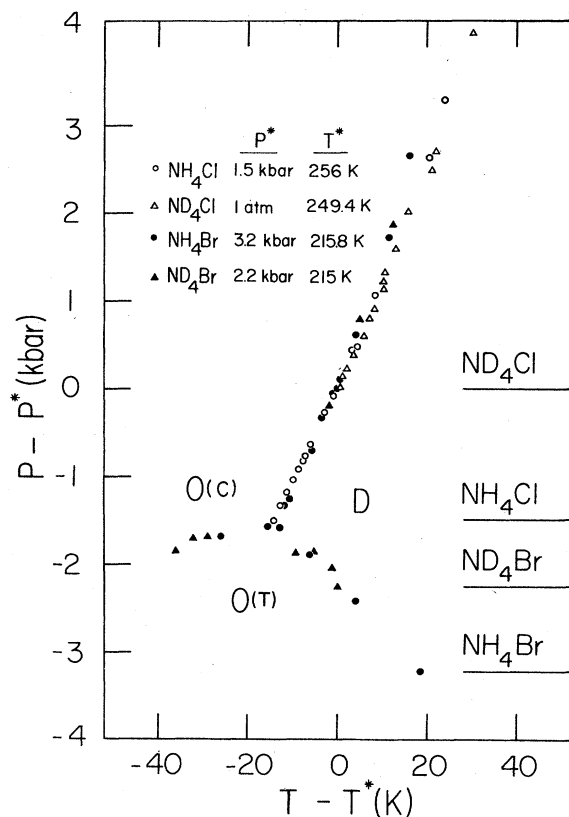


FIG. 7. Master phase diagram for ammonium chloride and bromide, where  $p^*$  and  $T^*$  represent the location of the D-O (C) multicritical point. The location of  $p=0$  for each salt is indicated along the right-hand side.

$\alpha_1$ .<sup>22</sup> Thus, it is difficult to decide on the quality of the agreement between the dynamical behaviors of  $\text{NH}_4\text{Br}$  and  $\text{NH}_4\text{Cl}$  at their D-O (C) multicritical points. There is, however, one feature of the  $\text{NH}_4\text{Br}$  attenuation that definitely does not fit the analogy with  $\text{NH}_4\text{Cl}$ . The ratio  $\alpha_o(\text{ordered})/\alpha_o(\text{disordered})$  at any given  $\Delta T$  is  $\sim 3.7$  for  $\text{NH}_4\text{Br}$  at 3.25 kbar, while this ratio is  $\sim 1.3$  for  $\text{NH}_4\text{Cl}$  at 1.5 kbar. The isobar at 3.25 kbar corresponds to a region of the phase diagram where the cubic ferro-order parameter should be dominant. For model A,  $z\nu=1.28$  at a second-order Ising fixed point and  $z\nu=1$  at a tricritical or higher-order point; but neither value agrees well with our experimental  $\theta(3.25 \text{ kbar})$ .

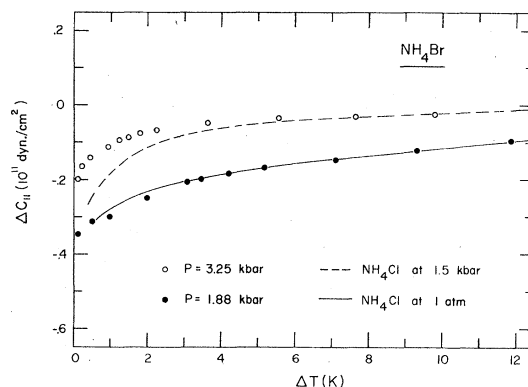


FIG. 8. Comparison of the elastic behavior of  $\text{NH}_4\text{Cl}$  and  $\text{NH}_4\text{Br}$  in the disordered phase. The quantity  $\Delta C_{11}$  is defined as  $C_{11} - C_{11}(255 \text{ K})$  for  $\text{NH}_4\text{Br}$  and  $C_{11} - C_{11}(285 \text{ K})$  for  $\text{NH}_4\text{Cl}$ . In each case,  $\Delta C_{11}$  corresponds to the difference between the  $C_{11}$  value at a given  $\Delta T = T - T_c(p)$  and the plateau value at  $\Delta T \approx 45 \text{ K}$ .

In summary, these acoustical measurements support a close analogy between the phase diagram of  $\text{NH}_4\text{Cl}$  and  $\text{NH}_4\text{Br}$ . Both crystals have a multicritical point along the D-O (C) transition line (at 1.5 kbar in  $\text{NH}_4\text{Cl}$  and 3.2 kbar in  $\text{NH}_4\text{Br}$ ), and the acoustical behavior of  $\text{NH}_4\text{Cl}$  at 1 atm is very similar to that of  $\text{NH}_4\text{Br}$  at a pressure (1.88 kbar) slightly above the triple-point pressure. This analogy explains the unusual behavior of  $\text{NH}_4\text{Cl}$  at 1 atm in terms of the effects of a "hidden" triple point at small negative pressures and the important role of competing interactions.

Theoretical progress in understanding both  $\text{NH}_4\text{Br}$  and  $\text{NH}_4\text{Cl}$  will require a compressible lattice model involving two order parameters—an  $n=1$  ferro-order parameter that is dominant at high pressures and an  $n=3$  antiferro-order parameter that plays an important role at low pressures.

#### ACKNOWLEDGMENTS

This work was supported in part by NSF Contract No. CHE-7520040. This work was also supported in part by Universidade de São Paulo, Brazil and in part by Fundação de Amparo à Pesquisa do Estado de São Paulo.

\*On leave from Universidade de São Paulo, Brazil.

<sup>1</sup>B. B. Weiner and C. W. Garland, *J. Chem. Phys.* **56**, 155 (1972), and references cited therein.

<sup>2</sup>C. W. Garland and C. F. Yarnell, *J. Chem. Phys.* **44**, 1112 (1966), and references cited therein.

<sup>3</sup>C. W. Garland and R. A. Young, *J. Chem. Phys.* **49**, 5282 (1968).

<sup>4</sup>Y. Ebisuzaki, *Chem. Phys. Lett.* **19**, 503 (1973).

<sup>5</sup>W. Press, J. Eckert, D. E. Cox, C. Rotter, and W. Kamitakahara, *Phys. Rev. B* **14**, 1983 (1976).

- <sup>6</sup>H. D. Hochheimer and T. Geisel, *J. Chem. Phys.* **64**, 1586 (1976).
- <sup>7</sup>W. Mandema and N. J. Trappenier, *Physica B* **81**, 285 (1976).
- <sup>8</sup>A. Hüller, *Z. Phys.* **254**, 456 (1972); **270**, 343 (1974); Y. Yamada, M. Mori, and Y. Noda, *J. Phys. Soc. Jpn.* **32**, 1565 (1972).
- <sup>9</sup>D. R. Nelson, J. M. Kosterlitz, and M. E. Fisher, *Phys. Rev. Lett.* **33**, 813 (1974); H. Rohrer, *ibid.* **34**, 1638 (1975); D. R. Nelson and E. Domany, *Phys. Rev. B* **13**, 236 (1976).
- <sup>10</sup>W. Mandema and N. J. Trappenier, *Physica* **76**, 102, 123 (1974).
- <sup>11</sup>C. W. Garland and C. K. Choo, *Phys. Rev. B* **8**, 5143 (1973).
- <sup>12</sup>C. W. Garland and R. J. Pollina, *J. Chem. Phys.* **58**, 5002 (1973).
- <sup>13</sup>H. Wagner and J. Swift, *Z. Phys.* **239**, 182 (1970); D. J. Bergman and B. I. Halperin, *Phys. Rev. B* **13**, 2145 (1976).
- <sup>14</sup>C. W. Garland and R. A. Young, *J. Chem. Phys.* **48**, 146 (1968).
- <sup>15</sup>It should be noted that in Ref. 3 the echo pattern was lost on going through the transition, whereas a continuous measurement of  $u_L$  was possible in the present work.
- <sup>16</sup>C. W. Garland and D. E. Bruins, *Phys. Rev. B* **12**, 2759 (1975).
- <sup>17</sup>M. Couzi, F. Danoyer, and M. Lambert, *J. Phys. (Paris)* **35**, 753 (1974).
- <sup>18</sup>C. W. Garland, G. Gorodetsky, and C. Zahradnik, *J. Chem. Phys.* **68**, 4771 (1978).
- <sup>19</sup>R. C. Leung, C. Zahradnik, and C. W. Garland, *Phys. Rev. B* (to be published).
- <sup>20</sup>K. K. Murata, *Phys. Rev. B* **13**, 4015 (1976).
- <sup>21</sup>P. C. Hohenberg and B. I. Halperin, *Rev. Mod. Phys.* **49**, 435 (1977).
- <sup>22</sup>It is not certain that there is any significance to the small difference in the exponents above and below  $T_c$  at 3.25 kbar. If  $\alpha_1$  were assumed to be zero below  $T_c$ , the resulting critical exponent in the ordered phase at 3.25 kbar would become 1.27. The data above  $T_c$  are much more sensitive to the presence of an  $\alpha_1$  contribution; if  $\alpha_1$  were set equal to zero,  $\theta$  in the disordered phase at 3.25 kbar would change from 1.2 to 1.0.
- <sup>23</sup>V. V. Prodnikov and G. B. Teitelbaum, *JETP Lett.* **23**, 296 (1976); E. D. Siggia and D. R. Nelson, *Phys. Rev. B* **15**, 1427 (1977).